Study of Gypsum Dehydration by Controlled Transformation Rate Thermal Analysis (CRTA)

E. Badens,* P. Llewellyn,† J. M. Fulconis,† C. Jourdan,* S. Veesler,*,1 R. Boistelle,* and F. Rouquerol‡

*Centre de Recherche sur les Mécanismes de la Croissance Cristalline—CNRS, Campus de Luminy, F-13288 Marseille cedex 9, France;
†Centre de Thermodynamique et de Microcalorimétrie—CNRS, 26, rue du 141ème R.I.A., F-13331 Marseille cedex 3, France; and
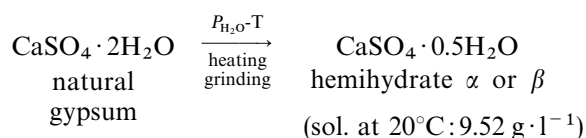‡Université de Provence, Case 2, Place Victor Hugo, F-13331 Marseille cedex 3, France

The dehydration of gypsum ($CaSO_4 \cdot 2H_2O$) into calcium sulfate hemihydrate ($CaSO_4 \cdot 0.5H_2O$) and anhydrites (γ-$CaSO_4$ and β-$CaSO_4$) was carried out by heating under a constant pressure of water vapor using Controlled transformation Rate Thermal Analysis. No intermediate formation of calcium sulfate hemihydrate occurred under a pressure of water vapor of 1 and 500 Pa (at the slow reaction rates used), whereas the transformation of gypsum into calcium sulfate hemihydrate was observed at 900 Pa. This transformation occurred without any lattice transformation when micron-sized needle-shaped crystals of gypsum were used, although a partial lattice transformation was observed when the starting sample was a centimeter-sized single crystal of gypsum. © 1998 Academic Press

INTRODUCTION

Set plaster is obtained from natural gypsum:

$$CaSO_4 \cdot 2H_2O \xrightarrow[\substack{\text{heating} \\ \text{grinding}}]{P_{H_2O}\text{-}T} CaSO_4 \cdot 0.5H_2O$$

natural gypsum → hemihydrate α or β

(sol. at 20°C: 9.52 g·l^{-1})

compact rock (or large single crystals) → powder

$$\xrightarrow[\substack{\text{dissolution/} \\ \text{crystallization}}]{H_2O} CaSO_4 \cdot 0.5H_2O \text{ gypsum}$$

(sol. at 20°C: 2.58 g·l^{-1})
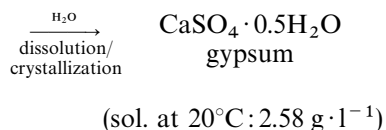
set plaster or gypsum powder
(depending on the relative proportions of water and hemihydrate)

[1]To whom correspondence should be addressed.

The mechanical strength of set plaster depends on the crystal habit and size, on the porosity, and also, quite strongly, on humidity. The mechanical strength of set plaster is weakened after adsorbing only a few percent of water, but it recovers its properties on desorption. The work of Coquard and Boistelle (1) showed that this dramatic effect of water does not result from gypsum solubilization in the presence of high relative humidity and led to the suggestion that it could be the result of water adsorption on the crystals of gypsum.
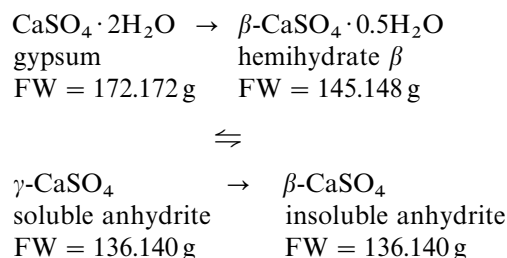
Set plaster consists of entangled crystals. Its cohesion and strength are the result of both this entanglement and inter-crystalline interactions. The faces of the crystals involved in these interactions are not the same from one crystal morphology to another. For example, for needle-shaped crystals, the faces involved are mainly (010), (120) and ($\bar{1}$11) in contrast to tabular crystals (grown in the presence of diethylene triamine pentaacetic acid) in which the faces involved are mainly (010), (120) and ($\bar{1}$01) (2). Therefore, as the relative proportions of the different faces are known, it is important to obtain information about adsorbed water to assess its role in these interactions. Several studies on gypsum dehydration were previously carried out (3–11), but water adsorption on gypsum crystals has not been studied. In order to study water adsorption on gypsum crystals, it is necessary to be able to define a reproducible surface state of the crystals (i.e., to be able to eliminate physisorbed species without affecting the chemical state of the surface). This is difficult because gypsum is thermodynamically unstable under vacuum, even at room temperature. It is for this reason, in this preliminary study, that we have used Controlled transformation Rate Thermal Analysis (CRTA) (12). This technique uses a feedback from the sample reaction itself to input into the algorithm governing the furnace control, thus allowing a decrease in the temperature and pressure gradients within the reacting sample which may often lead to irreproducibilities. This allows the preparation of a reproducible state to be defined before water adsorption studies.

The control obtained using CRTA permits a thermal pathway to be characterized at each point, not only by the sample temperature but also by the rate of reaction and, more importantly, by the gaseous environment (nature and concentration). This technique is thus also suited to an analytical study of the dehydration of gypsum crystals. Furthermore, it is also possible to control the residual pressure above the sample at different values so permitting an understanding of this latter parameter. This is the first time that such a technique has been employed on this material showing the progressive transformation of gypsum into other phases. Conventional thermogravimetric analysis of gypsum dehydration shows an apparent continuous water loss even when there is an intermediate partially dehydrated product (7).

EXPERIMENTAL

Generally, the thermal dehydration of gypsum is reported to lead to the formation of the following products:

$$CaSO_4 \cdot 2H_2O \quad \rightarrow \quad \beta\text{-}CaSO_4 \cdot 0.5H_2O$$
$$\text{gypsum} \qquad\qquad \text{hemihydrate } \beta$$
$$FW = 172.172\,g \qquad FW = 145.148\,g$$

$$\rightleftharpoons$$

$$\gamma\text{-}CaSO_4 \qquad\qquad \rightarrow \quad \beta\text{-}CaSO_4$$
$$\text{soluble anhydrite} \qquad \text{insoluble anhydrite}$$
$$FW = 136.140\,g \qquad\quad FW = 136.140\,g$$

γ-CaSO$_4$ is called soluble anhydrite because of its spontaneous hydration into hemihydrate under common atmospheric conditions and into gypsum upon immersion in water.

Sample

The set plaster and gypsum powder samples, both made of micron-sized needles of gypsum, were prepared from the dissolution of calcium sulfate hemihydrate β (provided by Lafarge) in water. The stoichiometric amount of water required to hydrate 1 g of hemihydrate is 0.186 g. Nevertheless, to obtain homogeneous samples of set plaster, it is necessary to first prepare homogeneous pastes with the hemihydrate powder. The Water/Hemihydrate (W/H) mass ratio used was equal to 0.6 to obtain our samples of set plaster and was equal to 20 to obtain gypsum powder. In this latter case, the hydration occurred without setting because of the large quantity of water. The average particle size is $15 \times 1.2 \times 1.2\,\mu m^3$ for set plaster and $18 \times 1.3 \times 0.7\,\mu m^3$ for gypsum powder. Set plaster is a porous cohesive material with a porosity of 57.7% (porous volume/overall volume) measured with a Purcell mercury porosimeter. We worked with mass of samples ranging from 20 to 105 mg. The

accurate composition of the initial calcium sulfate hemihydrate β is well known, and its purity is equal to 96%. The major impurity is calcium carbonate (2.5%). Single crystals of gypsum were centimeter-sized and of natural origin.

Apparatus and Methodology

The CRTA experimental setup is shown in Fig. 1. Sample A is located in a glass or fused-silica cell B which is itself in a refrigerated furnace C (allowing temperatures from 240 to 920 K). The sample temperature is measured by means of thermocouple D. Sample cell B is attached, by means of a Cajon VCR 1/4′ fitting, to the vacuum line which is exclusively made of all-metal high-vacuum elements. The vapor evolving from the sample flows through diaphragm G before reaching the pumping system I. At the start of each experiment, the pressure is lowered, by using pumping system I, from 10^5 Pa down to the desired value. The pressure is measured by Pirani gauges (PI 101 from Alcatel). The same pressure signal is sent to the heating controller of the furnace. The heating of the sample then takes place in such a way as to keep constant at a preset value the vapor pressure generated by the sample itself. Values of 1, 500, and 900 Pa were selected for the experiments reported here. With the preceding setup, maintaining a constant pressure measured by gauge F means maintaining a constant vapor flow through diaphragm G (since the vacuum available
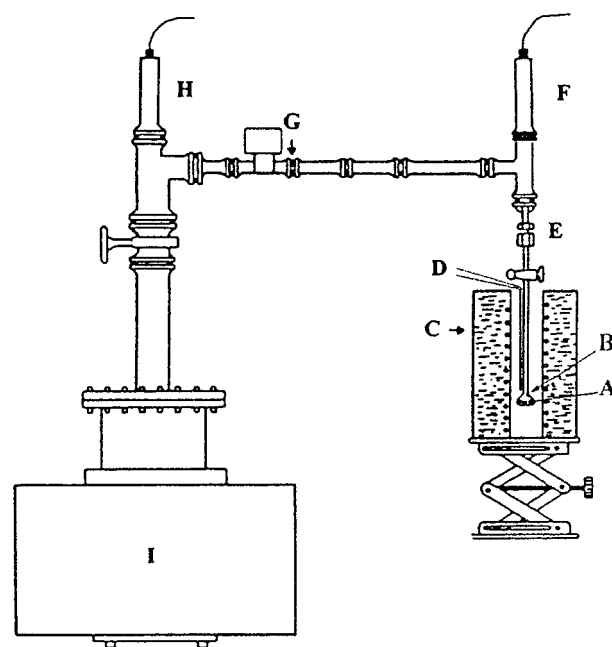

FIG. 1. Setup used for Controlled transformation Rate Thermal Analysis. A, sample; B, glass or fused-silica cell; C, Furnace; D, thermocouple; F and H, Pirani gauges; G, Diaphragm; and I, pumping system.

downstream is also constant). Because the whole vapor flow is the result of dehydration of the sample itself, the experiment is carried out not only under a constant residual vapor pressure of water but also at a constant rate of dehydration. The gas flow depends on the geometry of diaphragm G and on the pressure drop across it. As soon as the stationary state is attained, the gas flow, to the pumping system, is equal to the rate of production of the gaseous phase, which is thus constant. The degree of reaction is defined as 0 at the start of the reaction ($t = t_0$) and as 1 at the end of the step ($t = t_f$). Times t_0 and t_f are those when the preset residual pressure above the sample is reached and when the pressure drops, respectively. Reaction rate C, is expressed in h^{-1} [reciprocal of the time needed to complete the step: $C = 1/(t_f - t_0)$].

Because the dehydration is carried out at a constant rate, the length of each dehydration step varies linearly with the corresponding weight loss. Therefore, the plot of temperature versus time corresponds to a real thermogravimetric curve, $\Delta m = f(T)$, on which it is possible to identify each dehydration step.

Characterization of the Dehydration Products

Each gypsum sample contains a well-known amount of impurities (4%). Prior to the calculation of the weight loss resulting from water removal, we took into account this amount. Accordingly, the weight loss refers to pure gypsum. Furthermore, the sample of gypsum was weighed in the cell after the pressure had been lowered and before the temperature increased. At the end of the dehydration, the sample was also weighed in the closed cell in order to prevent spontaneous rehydration of the sample in contact with the humidity of the air. We tried to pour oil over the dehydration products to prevent them from rehydrating upon contact with air, but the products did not diffract enough to be resolved from the background because of oil diffusion. X-ray diffraction (XRD) studies were systematically carried out in order to characterize final products. The Debye–Scherrer diagrams were obtained using X rays with wavelength: $CuK\alpha_1 = 1.54056$ Å and an exposure of 16000 s. The detector used was an INEL CPS 120 system. The Laue diffraction diagrams have been taken with a Diffractis 581 apparatus (Enraf Nonius Delft). The crystal of gypsum of natural origin was mounted on a removable holder so that the b axis of the monoclinic crystal was parallel to the incident beam and perpendicular to the plane of the X-ray film.

RESULTS

The CRTA experiments were carried out under three different residual water vapor pressures: 1, 500, and 900 Pa.

CRTA at $P_{H_2O} = 1$ Pa

Figures 2, 3, and 4 represent the experimental CRTA curves obtained for the dehydration of three initial samples: 100 mg of a powder of gypsum needles (W/H = 20) at a rate of $0.015 \, h^{-1}$ (Fig. 2), 20 mg of set plaster (W/H = 0.6) at a rate of $0.010 \, h^{-1}$ (Fig. 3), and a 26.3 mg single crystal of gypsum obtained by cleavage of a natural sample at a rate of $0.015 \, h^{-1}$ (Fig. 4).

The three curves show only one dehydration step (part AB). The XRD analysis gave, for all three final products, the Debye–Scherrer diagram of β-CaSO$_4$ (Fig. 5). This is in good agreement with the mass analysis. The weight loss between point A and point B was about 20.9%, and the theoretical weight loss of water of recrystallization for the transformation of gypsum into anhydrite is 20.92%. No calcium sulfate hemihydrate was detected at this water vapor pressure of 1 Pa.

On the experimental curves, we observe a step at 840 K for gypsum powder (Fig. 2) and at 793 K for set plaster (Fig. 3). We can explain this step, which does not exist for pure single crystals, by the thermolysis of calcium carbonate. The hemihydrate used to obtain set plaster and gypsum powder contained about 2.5% of $CaCO_3$, so that we detected the removal of carbon dioxide. Surprisingly, we observed that the temperature of CO_2 removal is not the same for the two samples, whereas there is no difference in the temperature of water removal. Mineralogical properties of the sample can influence the temperature of decomposition (3). The temperature of water removal does not depend on these properties in our case but obviously the decomposition temperature of calcium carbonate does. We have no other experimental evidence for strengthening this interpretation.
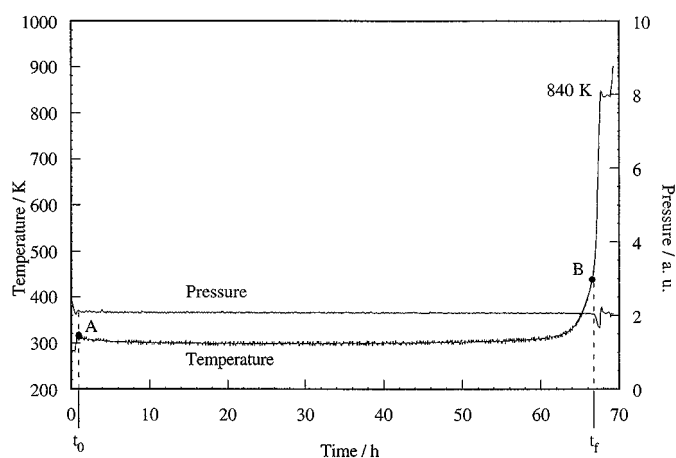

FIG. 2. Dehydration of a powder of gypsum needles (initial mass: 100 mg) (W/H = 20) at $P_{H_2O} = 1$ Pa at a reaction rate of $0.015 \, h^{-1}$.
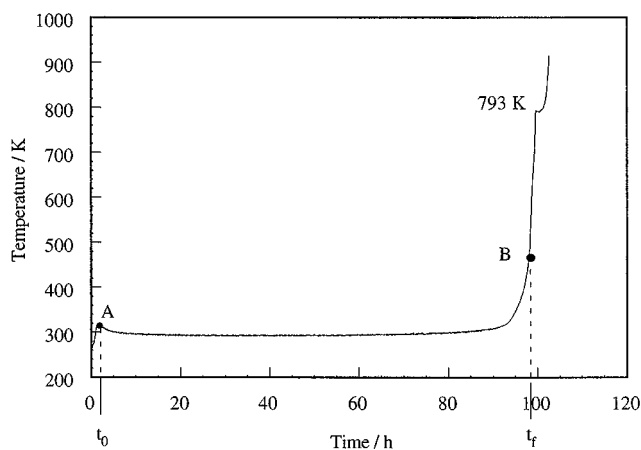
FIG. 3. Dehydration of set plaster (initial mass: 20 mg) (W/H = 0.6) at $P_{H_2O} = 1$ Pa at a reaction rate of $0.010 \, h^{-1}$.
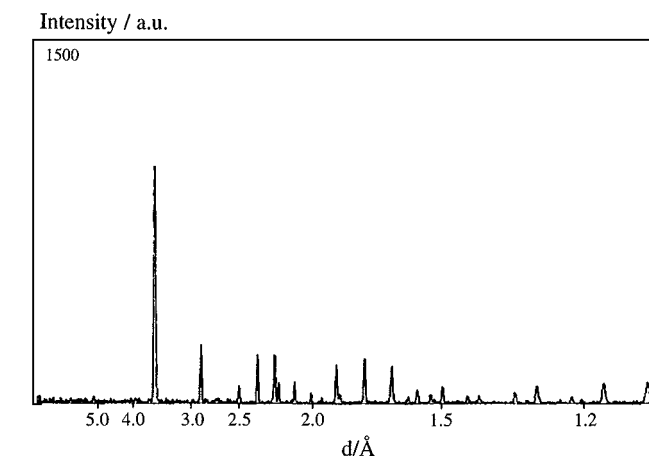

FIG. 5. Debye–Scherrer diagram of the final product of the dehydration of a single crystal of gypsum at $P_{H_2O} = 1$ Pa at a reaction rate of $0.015 \, h^{-1}$; Debye–Scherrer diagram of β-$CaSO_4$.

CRTA at $P_{H_2O} = 500 \, Pa$

Figure 6 represents the experimental CRTA curve obtained for a sample of 105 mg of set plaster (W/H = 0.6) at a rate of $0.014 \, h^{-1}$. The curve shows only one dehydration step (part AB). The XRD analysis of the final product gave the Debye–Scherrer diagram of β-$CaSO_4$ similar to the Debye–Scherrer diagram of Fig. 5. This is in good agreement with the mass analysis. The weight loss between point A and point B is about 20.9%. No calcium sulfate hemihydrate was detected at this water vapor pressure of 500 Pa.

CRTA at $P_{H_2O} = 900 \, Pa$

Initial Sample: Set Plaster (Micron-Sized Needles of Crystals of Gypsum). Figure 7 represents the experimental CRTA curve obtained for a sample of 100 mg of set plaster W/H = 0.6 at a rate of $0.022 \, h^{-1}$. The curve shows two

steps, between A and C at about 353 K and between C and E at about 381 K, which suggests the existence of two dehydration steps. The length ratio of 3/1 of step AC and step CE suggests that the first step corresponds to the transformation of gypsum ($CaSO_4 \cdot 2H_2O$) into calcium sulfate hemihydrate ($CaSO_4 \cdot 0.5H_2O$) (loss of 3/2 molecules of water) and that the second step corresponds to the transformation of calcium sulfate hemihydrate into anhydrite (γ-$CaSO_4$) (loss of 1/2 molecule of water).

The weight loss, 20.9% between point A and point E, indicates a complete removal of the crystallization water. From the XRD analysis carried out after the experiment, the final product was found to be γ-$CaSO_4$, although diffraction peaks of calcium sulfate hemihydrate (Fig. 8) were observed resulting from the spontaneous rehydration of γ-$CaSO_4$ into calcium sulfate hemihydrate.
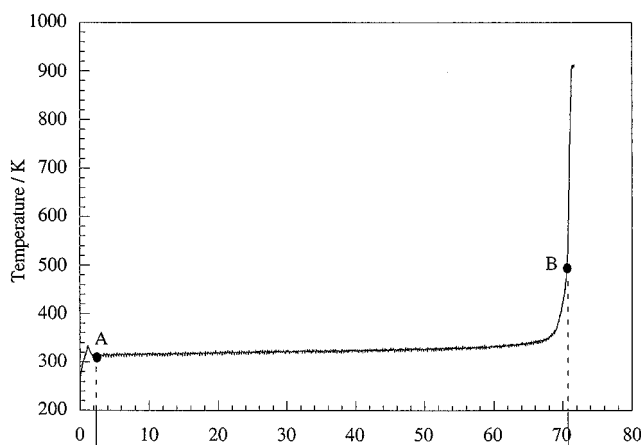

FIG. 4. Dehydration of a single crystal of gypsum (initial mass: 26.3 mg) at $P_{H_2O} = 1$ Pa at a reaction rate of $0.015 \, h^{-1}$.
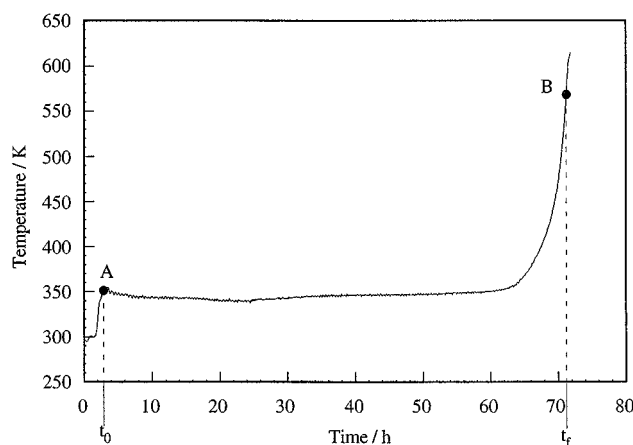

FIG. 6. Dehydration of set plaster (initial mass: 105 mg) (W/H = 0.6) at $P_{H_2O} = 500$ Pa at a reaction rate of $0.014 \, h^{-1}$.
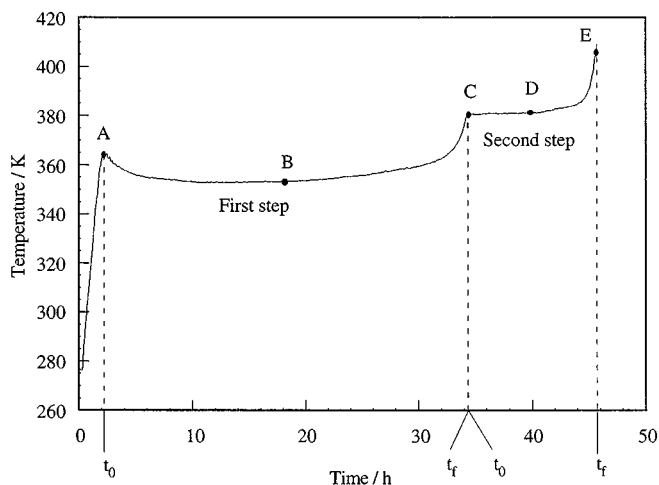
FIG. 7. Dehydration of set plaster (initial mass: 100 mg) (W/H = 0.6) at P_{H_2O} = 900 Pa at a reaction rate of $0.022\,h^{-1}$.

FIG. 9. Debye–Scherrer diagram made at point D of the curve showed in Fig. 7. It corresponds to a mixture of gypsum and hemihydrate.

A Debye–Scherrer diagram of the sample made at point D of the curve shown in Fig. 7 corresponds to a mixture of gypsum and calcium sulfate hemihydrate (Fig. 9), whereas we expected not to find gypsum, the curve showing the end of the first step of dehydration. Calcium sulfate hemihydrate resulted from the spontaneous transformation of γ-CaSO$_4$ into calcium sulfate hemihydrate as soon as the material was exposed to air after the experiment. We carried out X-ray phase analysis based on the dependence of the intensity of reflection on the contents of the corresponding phase. We used a peak decomposition program DECOMPXR (13) which provided us with accurate information, intensity of the peaks associated with all the phases present in the sample. We found 55% of hemihydrate and 45% of gypsum.

Initial Sample: Single Crystal of Natural Gypsum (Centimeter-Sized). At P_{H_2O} = 900 Pa and at a rate of $0.023\,h^{-1}$, we obtained a similar experimental CRTA curve to the previous sample of set plaster made of micron-sized needles of gypsum of Fig. 7. Before the CRTA experiment, we took two Laue diffraction diagrams, one with a ponctual beam (Fig. 10) and another one with a beam with a large rectangular cross section (Fig. 11). From the Cole and Lancuki data (14), we have simulated the Laue diffraction diagram (Fig. 12). The comparison between Fig. 12 and Fig. 10 shows that the structure of gypsum crystal is in good agreement with the unit cell proposed by Cole and Lancuki. We stopped the CRTA experiment, at a first point approximately at the middle of the dehydration step of gypsum into hemihydrate
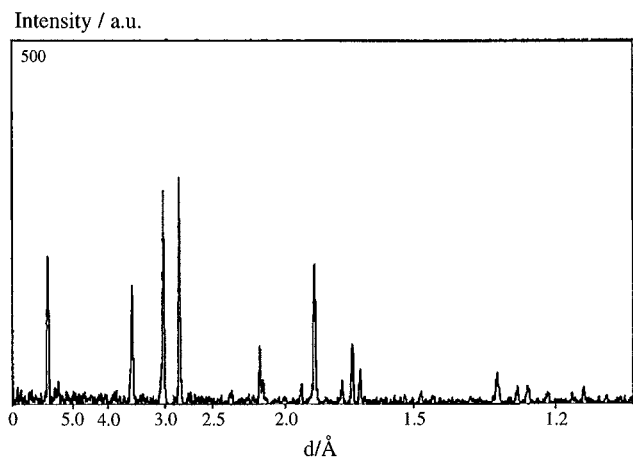

FIG. 8. Debye–Scherrer diagram of the final product of the dehydration of set plaster (W/H = 0.6) at P_{H_2O} = 900 Pa at a reaction rate of $0.022\,h^{-1}$; Debye–Scherrer diagram of hemihydrate β.
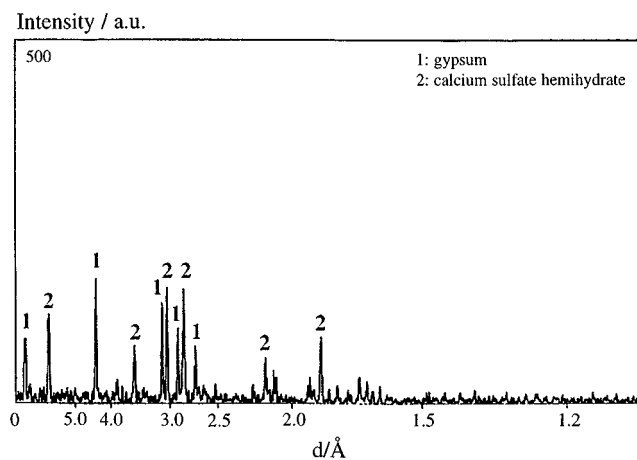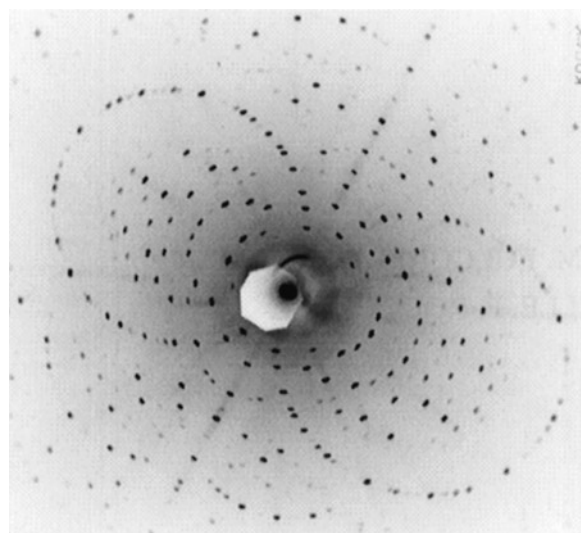

FIG. 10. Laue diffraction diagram (ponctual beam) of the single crystal of gypsum taken before the CRTA experiment.

FIG. 11. Laue diffraction diagram (beam with a large rectangular cross section) of the single crystal of gypsum taken before the CRTA experiment.

FIG. 13. Laue diffraction diagram (beam with a large rectangular cross section) of the dehydration product taken point B of the curve showed in Fig. 7.

(point B of Fig. 7). At this stage, we observed a water loss of 11% and a Laue diffraction diagram taken with a beam with a large rectangular cross section (Fig. 13) showed that the sample was still a single crystal. We continued the experiment and stopped again at a moment corresponding to a loss of water of 15.7% and consequently to the end of the dehydration of gypsum into calcium sulfate hemihydrate (point C of Fig. 7). The Laue diffraction diagram realized at point C shows locally reinforced Debye–Scherrer rings characteristic of a texture made of a multitude of small crystals with a preferred orientation (15). This preferred orientation of the polycrystalline dehydration phase in the

crystal parent was already observed and interpreted by Richards (4) concerning the transformation of gypsum into calcium sulfate hemihydrate or into anhydrite. In this study, we did not investigate the texture. In order to characterize the crystalline structure of the small crystals, we made a Debye–Scherrer diagram. Because of the orientations of small crystals and because the specimen was not rotated about its own axis during the experiments, we did not observe simultaneously all the diffraction hkl reflections as in the case of "true" powder diagram. Depending on the zone observed on the sample, we obtained either diffraction of hkl planes of calcium sulfate hemihydrate or diffraction of hkl planes of gypsum. The Debye–Scherrer diagram obtained was of poor quality, showing a poorly crystallized material. These results showed that the lattice transformation of the initial single crystal was incomplete.

DISCUSSION

Transformation of Gypsum into Calcium Sulfate Hemihydrate

Because at point D on the curve in Fig. 7 the dehydration of gypsum into calcium sulfate hemihydrate is complete, whereas the Debye–Scherrer diagram shows a mixture of gypsum and hemihydrate (Fig. 9), a solid/solid transformation of gypsum into calcium sulfate hemihydrate occurred without a lattice transformation. The gypsum as final product cannot result from a rehydration of calcium sulfate hemihydrate because we strongly controlled the mass of the product when the sample was brought back to atmospheric conditions prior to XRD analysis. A rehydration of hemihydrate would result in an increase of the mass of about

FIG. 12. Laue diffraction diagram of a single crystal of gypsum simulated from Cole and Lancuki data.

8 mg which would have been detected. During the XRD analysis, adsorption of water was not observed in the Debye–Scherrer diagram.

If the gypsum lattice as the final product lattice does not result from the rehydration of calcium sulfate hemihydrate and if the dehydration of gypsum has been complete, this study reveals that there is a transformation of gypsum into calcium sulfate hemihydrate without lattice transformation in the case of micron-sized needles of gypsum dehydration and with a partial lattice transformation in the case of single-crystal dehydration. This part of the study needs more precise investigation. For our part, we can just notice that the lattice transformation of gypsum into calcium sulfate hemihydrate involves important changes even if they both crystallize in the monoclinic system (Table 1). So, if the dehydration occurs very slowly, in a "soft chemistry" manner as induced by CRTA, it is not surprising to keep the initial lattice. A topotactic transformation of gypsum into hemihydrate was often assumed (10, 11) but not really demonstrated. Conversely, there is more information about the topotactic transformation of hemihydrate into gypsum (17–19). In the present study, because a topotactic transformation is assumed to be a solid phase chemical reaction which leads to a material with crystalline orientation related to the orientations of the initial product (20), a topotactic transformation without lattice transformation under the conditions of our study and with micron-sized needle-shaped crystals of gypsum is proposed. We observed a partial lattice transformation with the centimeter-sized single crystal. The size of the crystal makes such a difference because water removal creates more stresses in a centimeter-sized crystal than in a micron-sized one.

Transformation of γ-CaSO$_4$ into β-CaSO$_4$

The transformation of γ-CaSO$_4$ into β-CaSO$_4$, already studied by several authors (3, 5–8), occurs somewhere between 400 and 500 K. Under our experimental conditions (residual water vapor pressure of 1 Pa, reaction rate of 0.020 h^{-1}), it takes place at 423 K (Fig. 14). This is determined by a small peak in the CRTA curve: the exothermic recrystallization accelerates gas evolution from the sample (sharply because of self-heating and because of a weakening
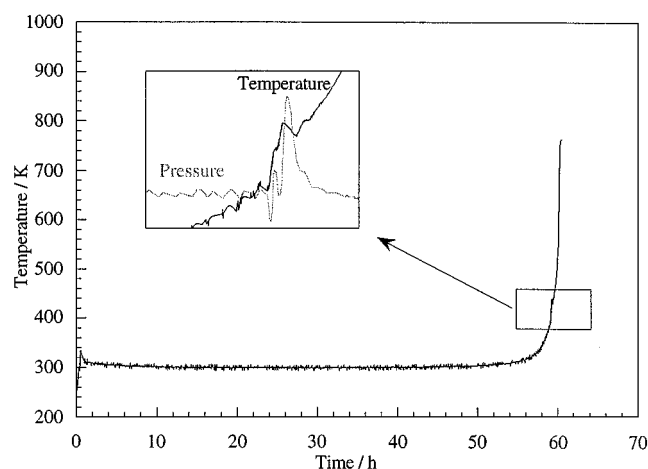

FIG. 14. Dehydration of a powder of gypsum needles (initial mass: 100 mg) (W/H = 20) at $P_{H_2O} = 1$ Pa at a reaction rate of 0.020 h^{-1}.

of water bonding in the solid during its reorganization) so that the CRTA control loop tends to cool down the sample. A similar phenomenon was observed, again by CRTA, for the dehydration of a zirconia gel (23). In general, the existence and position of the perturbation not only depends on vapor pressure and reaction rate but also on the crystalline structure, thermal conductivity, and impurity content.

CONCLUSION

Depending on water vapor pressure, the thermal path varies, and consequently the dehydration products also vary. At 500 Pa or below, there is only one dehydration step from gypsum to γ-CaSO$_4$. At 900 Pa, calcium sulfate hemihydrate is an intermediate product between gypsum and γ-CaSO$_4$. An original result of this study is that, depending on the microstructure of the initial sample of gypsum, the lattice of the intermediate calcium sulfate hemihydrate varied. There is no transformation of the gypsum lattice in the case of micron-sized needles of gypsum, and there is a partial transformation in the case of centimeter-sized single crystals of gypsum.

Future work will concern CRTA experiments at higher water vapor pressure, above 900 Pa, in order to observe the

TABLE 1
Data on the Crystal Lattice of the Different Calcium Sulfates

	Matrix	a (Å)	b (Å)	c (Å)	α (°)	β (°)	γ (°)	Cell volume (Å^3)	Cell content
CaSO$_4 \cdot$ 2H$_2$O (14)	Monoclinic	5.670	15.201	6.533	90	118.6	90	494.37	4(CaSO$_4 \cdot$ 2H$_2$O)
CaSO$_4 \cdot$ 5H$_2$O (21)	Monoclinic	12.019	6.930	12.670	90	90.23	90	1055.30	12(CaSO$_4 \cdot$ 5H$_2$O)
γ-CaSO$_4$ (21)	Orthorhombic	12.077	6.972	6.304	90	90	90	530.80	6(CaSO$_4$)
β-CaSO$_4$ (22)	Orthorhombic	7.006	6.998	6.245	90	90	90	306.18	4(CaSO$_4$)

removal of adsorbed water which would appear in Fig. 7 in the first part of the variation of temperature before point A.

REFERENCES

1. P. Coquard and R. Boistelle, *Int. J. Rock. Mech. Min. Sci & Geomech. Abstr.* **31** (5), 517 (1994).
2. L. Amathieu and R. Boistelle, *J. Crystal Growth* **79,** 169 (1986).
3. M. Murat and M. Foucault, "Calcium Sulfates and Derived Materials." R.I.L.E.M. International Symposia, Lyon, 1977.
4. K. J. Richards, *J. Am. Ceram. Soc.* **49,** 342 (1966).
5. C. A. Strydom, D. L. Hudson-Lamb, J. H. Potgieter, and E. Dagg, *Therm. Acta* **269/270,** 631 (1995).
6. D. L. Hudson-Lamb, C. A. Strydom, and J. H. Potgieter, *Therm. Acta* **282/283,** 483 (1996).
7. A. Putnis, B. Winkler, and L. Fernandez-Diaz, *Mineral. Mag.* **54,** 123 (1990).
8. G. A. Lager, Th. Armbruster, F. J. Rotella, J. D. Jorgensen, and D. G. Hinks, *Am. Mineral.* **69,** 910 (1984).
9. S. Stenström and L. Nilsson, *Zem-Kalk-Gips* **9,** 478 (1992).
10. O. W. Flörke, *Neus J. b. Miner. Abh.* **84,** 189 (1952).
11. M. Goto and M. J. Ridge, *Aust. J. Chem.* **18,** 769 (1965).
12. J. Rouquerol, *Therm. Acta* **144,** 209 (1989).
13. B. Lanson and D. Champion, *Am. J. Sci.* **291,** 473 (1991).
14. W. F. Cole and C. J. Lancuki, *Acta Cryst.* **B30,** 921 (1974).
15. B. K. Vainshtein, "Modern Crystallography I." A. A. Chernov, L. A. Shuvalov, 307, M. Cardona, P. Fulde, H.-J. Queisser, Springer—Verlag, 1981. [Springer Series in Solid-State Sciences, Vol. 15]
16. G. Pacheco and M. Portilla, *Materiales de construccion* **41** (222), 27 (1991).
17. E. Eipeltauer, *Zem-Kalk-Gips* **16,** 9 (1963).
18. K. W. Fisher, "Wissenschaftliche zeitschrift der hochschule fur architektur und bauwesen weimar." **3,** 1963, pp. 351.
19. R. J. Ridge and J. Beretka, *Rev. Pure Appl. Chem.* **19,** 17 (1969).
20. A. Deschanvres and B. Raveau, *Rev. Chim. Miner.* **5,** 201 (1968).
21. C. Bezou, J. C. Mutin, and A. Nonat, *J. Chim. Phys.* **87,** 1257 (1990).
22. Personal communication, M. Sipple and J. C. Mutin, University of Bourgogne, LRRS–CNRS, Dijon, France 1 (1997).
23. M. J. Torralvo, Y. Grillet, F. Rouquerol, and J. Rouquerol, *J. Chim. Phy.* **77** (2), 125 (1980).